Electromagnetic Field Evaluation of a 500kV High Voltage Overhead Line

Shadreck Mpanga[1], Wang Feng[1], Chen Chun[1]
[1]College of Electrical and Information Engineering, Hunan University, Changsha, P.R. China 410082
Corresponding author: shadreck.mpanga@gmail.com, wangfeng@263.net, chch3266@126.com

Abstract

Many scientific articles have been written about electromagnetic field distributions under high voltage overhead transmission lines. However, some readers are still left wondering just how exactly the distribution curves formed by the fields are related to the mathematical models used. This paper presents case study results of a 500kV alternating current overhead transmission line, and explicitly shows how the fields vary under high voltage lines by employing easily understood mathematical models. The numerical simulations, done using MATLAB, can help anyone willing to evaluate the amount of electromagnetic fields available under any other high voltage overhead transmission line. The magnitudes of the fields obtained are compared with the standard values set by the International Radiation Protection Agency so as to assess the integrity of external insulation of the line. Thus, the technical staff can easily attend to complaints that may arise about the electromagnetic field effects from the line.

Keywords: Electromagnetic fields, Insulation, Electrical accidents, MATLAB, Numerical simulation

1. Introduction

Electricity is such an essential commodity of modern civilization that everybody is exposed to some form of electromagnetic field. These fields are spread all the way from power generation stations via overhead transmission conductors to energy utilization areas where, even if underground cables [1] may be used, electromagnetic fields can still be detected on the ground surface. The strongest electric fields are encountered in the transmission corridor of high voltage overhead transmission lines, especially during overvoltage [2] conditions. The electric fields, produced by the power system's voltage, can be a source of electrical accidents if not properly analyzed and understood. Magnetic fields emanate from the power system's current and may not be as strong in the transmission corridor as they are in utilization areas with a population of large electric motors.

Many articles [3-8] have been written about the distribution of electromagnetic fields under high voltage overhead transmission lines. The articles have usually concentrated on either magnetic fields alone or electric fields alone. The methods employed in these articles still leave some readers wondering just how exactly the electromagnetic field curves produced directly relate to the mathematical models used. Never in any of these articles has the longitudinal distribution of the electromagnetic field on the ground level been explained. Only the lateral profile of the electromagnetic field distribution on the ground has been explained in the already published literature.

This paper aims at bridging the above gap by explicitly showing a more practical approach on how the maximum charge values are obtained from the overhead line geometric dimensions and its highest rated system voltage. Using these charges, the overhead conductor surface voltage gradient and the ground level distribution of electric field for both the lateral and longitudinal profiles are evaluated. From the overhead line geometric dimensions and system current flows, the magnetic field intensity distribution on the ground is as well clearly obtained for both the lateral and longitudinal profiles. Hence, it is explained how electric fields arise from electric charges and how magnetic fields arise from the motion of these electric charges. This has been done by way of numerical simulations, in MATLAB, of a case study of a 500kV AC 400km long overhead transmission line.

External insulation limits are of interest in this paper. Thus, we decided to evaluate the electromagnetic field distributions on the ground level and not one meter above ground as it is commonly done. Line insulation starts from knowing the actual electric field on the conductor surface and that on the ground. The nature of conductor sag [9, 10] of high voltage overhead lines necessitated the need to evaluate both the lateral and the longitudinal profiles of electromagnetic field distributions within the transmission line corridor starting from the position of largest sag. This is the region prone to electrical accidents due to clearance infringements.

Although a rigorous treatment of the mathematical models used herein is given in [11], we strongly believe that the manner in which they have been applied for numerical simulations in this paper will address questions that are of interest to anyone attempting to evaluate the amount of electromagnetic fields available under any other high voltage overhead line.

2. Mathematical Models for High Voltage Overhead Line External Insulation
2.1. Conductor Surface Voltage Gradient

To find the conductor surface voltage gradient, equation (1) is first used to derive the 3×3 inverse matrix [M] from the Maxwell's potential coefficients matrix [P], which is calculated from the overhead line geometric dimensions. This inverse matrix is then applied in equation (3) for the derivation of charges sustained on the three overhead line conductors. A horizontal three-phase configuration is assumed for the work in this paper as figure 1 shows.

$$[M] = [P]^{-1} \tag{1}$$

In conjunction with figure 1, the entries of equation (1) are as follows:

$$P_{11} = P_{22} = P_{33} = \ln\left(\frac{2H}{r_{eq}}\right), \quad P_{13} = P_{31} = \ln\left(\frac{\sqrt{4H^2 + 4S^2}}{2S}\right), \quad P_{12} = P_{21} = P_{23} = P_{32} = \ln\left(\frac{\sqrt{4H^2 + S^2}}{S}\right)$$

Note that phases A, B, and C respectively refer to 1, 2, and 3 in these entries. H is the conductor height in meters, S is conductor spacing in meters, r_{eq} is given in equation (2) and is the equivalent radius of the conductor bundle in meters.
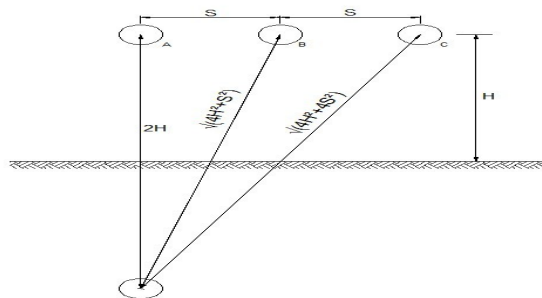
Figure 1. Three-Phase Horizontal Configuration of an Overhead Transmission Line

Equation (2) shows bundle radius R ($R = B/\sqrt{3}$ in this paper, B is bundle spacing), number of conductors in a bundle N, and radius of sub-conductor r.

$$r_{eq} = R * (N * r / R)^{1/N} \tag{2}$$

when the three conductors experience a balanced positive-sequence voltage excitation under steady-state, a matrix of charges [Q] can be derived as shown in equation (3), where V is rms value of line-to-ground voltage and , i=1, 2, 3 for i^{th} row.

$$\frac{Q_i}{2\pi e_0} = \sqrt{2}V \left[m_{i1}^2 + m_{i2}^2 + m_{i3}^2 - \left(m_{i1}m_{i2} + m_{i2}m_{i3} + m_{i3}m_{i1} \right) \right]^{0.5} \tag{3}$$

Equation (4) is then used to evaluate the electric field *E* on conductor surface.

$$E = \frac{Q_i}{2\pi e_0} * \frac{1}{N} * \frac{1}{r} * \left[1 + \left(N - 1 \right)\frac{r}{R} \right] \tag{4}$$

For respective maximum electric field expressions, E_{op} and E_{cp}, for any point *p* on outer conductor surface and on center conductor surface, equations (5) and (6) can be used.

$$E_{op} = \frac{1 + \left(N - 1 \right)r / R}{N * r * \ln \left\langle \frac{2H}{r_{eq}} * \frac{1}{\left[\left\{ 1 + \left(2H / S \right)^2 \right\} \left\{ 1 + \left(H / S \right)^2 \right\} \right]^{0.25}} \right\rangle} V \tag{5}$$

$$E_{cp} = \frac{1 + \left(N - 1 \right)r / R}{N * r * \ln \left\langle \frac{2H}{r_{eq}} * \frac{1}{\left[\left\{ 1 + \left(2H / S \right)^2 \right\} \right]^{0.5}} \right\rangle} V \tag{6}$$

Equations (1) through (6) stipulate that with only the knowledge of an overhead line geometric dimensions and the system's highest rated voltage, it is possible to determine the maximum conductor surface voltage gradient.

2.2. Ground Level Electric Field Distribution

The three-phase overhead line conductors can attract either (+q, +q, +q), (+q, 0, -q) or (+q, -2q, +q) charge conditions. These *three scenarios* respectively lead to the mathematical models for ground level electric field E_v distributions indicated by equations (7), (8) and (9).

$$E_v^1 = \frac{Q}{\pi e_0 H} \left[\frac{1}{1 + \left(d + S \right)^2 / H^2} + \frac{1}{1 + d^2 / H^2} + \frac{2}{1 + \left(d - S \right)^2 / H^2} \right] \tag{7}$$

$$E_v^2 = \frac{Q}{\pi e_0 H} \left[\frac{1}{1 + \left(d - S \right)^2 / H^2} - \frac{1}{1 + \left(d + S \right)^2 / H^2} \right] \tag{8}$$

$$E_v^3 = \frac{Q}{\pi e_0 H} \left[\frac{1}{1 + \left(d + S \right)^2 / H^2} + \frac{1}{1 + \left(d - S \right)^2 / H^2} - \frac{2}{1 + \left(d / H \right)^2} \right] \tag{9}$$

In equations (7) through (9), *d* is the lateral distance from the centre phase towards corridor edge. The factor $Q/\pi\varepsilon_0$ is obtained from equation (3). Only the vertical component E_v is evaluated as its horizontal component is zero on an equipotential ground.

2.3. Ground Level Magnetic Field Distribution

The horizontal component of the magnetic field intensity H_{HZ} in equation (10) is used since its vertical component is zero as the ground surface is assumed to be a flux line. In transmission circuits, currents are usually balanced. Hence, the phases A, B, and C respectively have $I_a = I\angle0^0$, $I_b = I\angle-120^0$ and $I_c = I\angle-240^0$ currents flowing through them. The other parameters are as defined in equations (7) through (9).

$$H_{HZ} = \frac{HI_a}{\pi\left[(d+S)^2 + H^2\right]} + \frac{HI_b}{\pi\left(d^2 + H^2\right)} + \frac{HI_c}{\pi\left[(d-S)^2 + H^2\right]} \qquad (10)$$

Equations (1) through (10) can now be applied in electromagnetic field measurements for a real-life situation captured in the following section. These mathematical models can prove very handy even without the measuring instruments available on the market.

3. A 400 km 500 kV AC Overhead Line Model
3.1. Overhead Line Data Gathered

The following is the overhead line geometric data: conductor height H 27m, conductor spacing S 13m, average span length between any two towers 345m, conductor diameter 28.62mm, conductor bundle spacing 45cm, and overhead line corridor width 70m. Table 1 contains measured data while on site.

Table 1. Measured Parameters while on Site

Ambient Temp.(^{0}C)	Conductor Temp.(^{0}C)	Load Current (A)	Conductor Sag (m)	Wind Speed (m/s)
28.7	31	445	13.36	1.4
28.7	30.8	439	13.2	1.4
29.6	31.9	530	13.48	2.4
29.6	31.2	523	13.28	2.4

3.2. Overhead Line Modeling

The overhead line data were fed into a Power line parameter calculation program in MATLAB. The positive sequence inductance came out as 0.963mH/km, positive sequence resistance 0.0224ohm/km, and positive sequence capacitance 12.1 nF/km. Figure 2 shows the 500kV, 50Hz AC, 400km high voltage overhead transmission line model.

The objective of the model is to simulate, using SimPowerSystems software in MATLAB, the actual situation that residents near the overhead transmission line corridor are exposed to on a typical day.
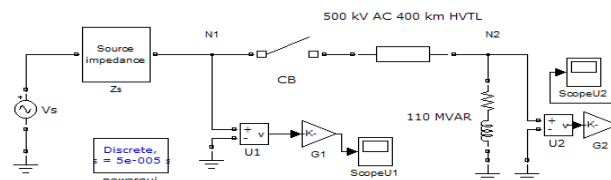
Figure 2. Distributed parameter model of a 500 kV AC overhead line.

From voltage stability point of view, reactive power compensation of 110 MVAR was used at the end of the line to maintain sending end and receiving end voltage within the range 500-525kV.

4. Results and Analysis
4.1. Conductor Surface Voltage Gradient
Conductor surface voltage gradients for the outer and center conductors were calculated using equations (5) and (6) respectively, and results were recorded in Table 2.

Table 2. Conductor Surface Voltage Gradients

At height 27 m (kV/cm)		At height 18.2 m (kV/cm)		At height 13.8 m (kV/cm)	
Centre Phase	Outer Phase	Centre Phase	Outer Phase	Centre Phase	Outer Phase
17.46	16.35	17.60	16.58	17.76	16.86

From the values in Table 2, it could be seen that the conductor surface voltage gradients of the studied line tie in well with the values accepted in many countries worldwide for prevention of corona discharge. This was confirmed by using corona-inception surface voltage gradient equation, $E_O = \dfrac{2192\delta}{m}\left(1 + 0.0308/\sqrt{r_c\delta}\right)\ kV/m,\ r.m.s,$ where δ is air density factor, m is roughness factor, and r_c is sub-conductor radius in a bundle in meters. The configuration of the transmission line in the case study reveals that corona-inception surface voltage gradient is 20kV/cm. The values in Table 2 are all lower than this value.

It was further observed that conductor surface voltage gradient increases with decreasing conductor height. Hence, there is need to observe minimum conductor-ground clearance. The specified conductor-ground clearance for a 500kV AC overhead line by the National Electrical Safety Council is 10.668m. The transmission line in this case study had a conductor height of 13.52m at mid span when the maximum sag of 13.48m (recorded in Table 1) was observed.

It must be noted that the maximum of 525kV line-to- line voltage was divided by the factor $\sqrt{3}$ for the phase-to-ground voltage used to calculate the values in Table 2. In a typical situation, the surface voltage gradients are less than these values. From the corona eruption point of view, the line external insulation [11, 12] of the studied transmission line can be said to be technically sound.

4.2. Ground Level Electromagnetic Fields
By letting E vary with d in equations (7) through (9), the lateral profiles of ground level electric fields were obtained and shown in figure 3. Making E vary with H in the same equations for one span between two towers made it possible to obtain the longitudinal profiles of ground level electric field distributions shown in figure 4. The conductor height H was varied from 13.2m (mid span height) to 27m (conductor height at the tower).
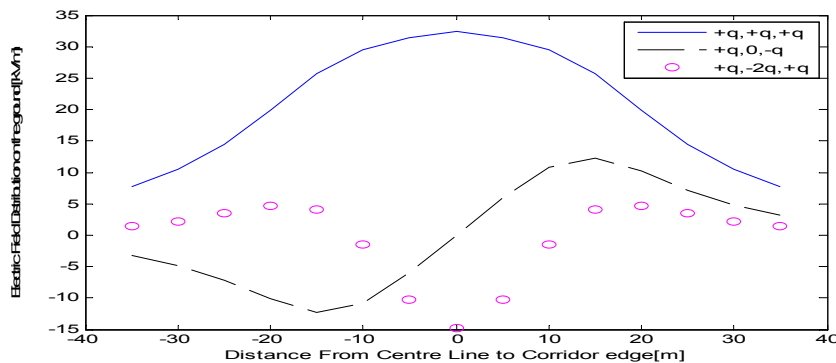
Figure 3. Lateral profile of electric field distribution on the ground

By letting H_{HZ} vary with d in equation (10), the lateral profiles of ground level magnetic fields for the typical loads and full load were obtained and shown in figure 5 (a). Making H_{HZ} vary with H in the same equation for one span between two towers made it possible to obtain the longitudinal profiles of ground level magnetic field distributions shown in figure 5 (b). The conductor height H was varied from 13.2m (mid span height) to 27m (conductor height at the tower). Only the 530A load current was chosen for the longitudinal profile.

The numerical simulations in figure 3 reveal that the electric field (32.38kV/m) directly under the line for the charge scenario, (+q, +q, +q), is slightly higher than that set by the international radiation protection agency (IRPA) of 30kV/m for short time exposure of electrical personnel. It is not ideal for the public. The magnitudes of the other two charge scenarios, (+q, 0, -q) and (+q, -2q, +q), are less than or equal to 15kV/m directly under the transmission line. These fall within the accepted range by the IRPA for short time and long term exposure of both the electrical personnel in protective clothing and the general public. The simulations in figure 4 are a cross-section of the lateral profile shown in figure 3. They show the effect of sag on the magnitude of the electric field present on the ground. It is observed that the field is stronger at the mid span than at the towers on horizontal ground. This depicts a direct correlation of the electric field with conductor height.

(a) Outer Phase　　　　　　　(b) Centre Phase
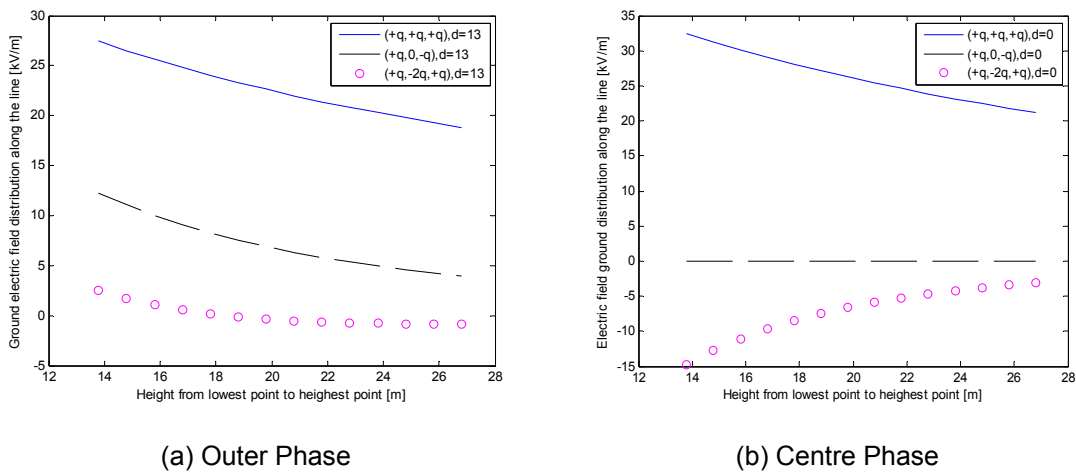
Figure 4. Longitudinal Profile of Electric Field Distribution on The Ground

(a) Lateral profile　　　　　　　(b) Longitudinal profile for 530 A load
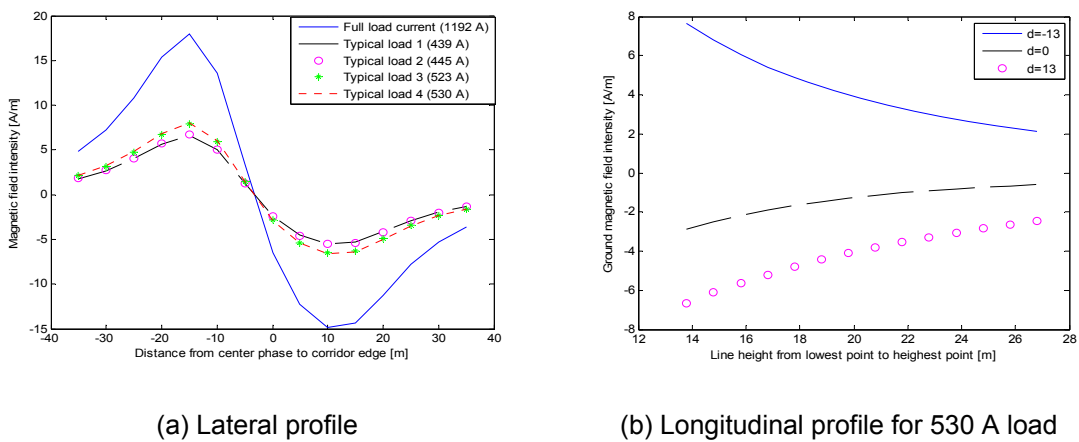
Figure 5. Magnetic Field Distribution Patterns on The Ground

When full load current (1192 A) flows in the system, the ground level magnetic field as shown in figure 5 (a) has the maximum absolute value of 17A/m. This corresponds to a value of 0.0214mT for magnetic flux density. The value set by IRPA as a safety guide for the general public is 0.2mT. Thus, from magnetic field viewpoint, the external insulation of the power line in the case study is satisfactory. In fact, in most cases as can be inferred from figure 5 (a), typical loads give rise to magnetic fields less than that of the full load current. Figure 5(b) is a cross-section of the ground level magnetic field produced in figure 5 (a) for a current of 530 A through the system. It can also be observed that the absolute value of the magnetic field on the ground decreases with increasing conductor-ground clearance as one move from the mid section of the line towards the tower on either side. In fair weather throughout the line, this situation can prevail on every other span.

4.3. Switching Transients

By interfacing the output voltage of figure 2 with the mathematical models used for calculating the electromagnetic fields on the ground, electromagnetic transients were simulated during a switching operation. This was done for the first250 ms of switching at positions d=0 (directly under centre phase) and d=35m (corridor edge) and results were recorded in figure 6. The figures show that ground level electric fields are also sinusoidal with time and increase in amplitude during a 5 cycle switching voltage transient before reverting to their steady state values. The transient fields are on the higher side and can be a source of electric shock on human beings who may happen to be under the line during this time.

(a) centre phase   (b) corridor edge
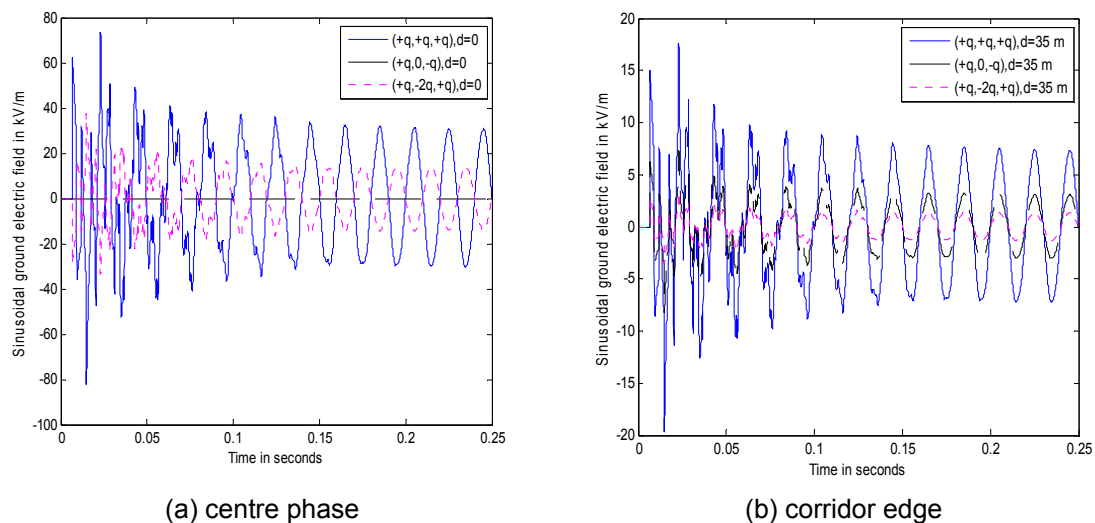
Figure 6. Electric Field Transients Development During a Switching Operation

From Ampere's circuital law with Maxwell's correction, it can be inferred from figure 6 that the quantities are varying electric fields with time, which can give rise to magnetic fields. Thus, the magnetic field transients also follow a similar pattern as that of the electric field transients.

It must be noted that, in order to increase human safety, the International Commission on Non-ionizing Radiation Protection uses a factor of 10 to derive occupational limits for electrical personnel and a factor of about 50 to arrive at exposure limits for the general public. Thus, transients that last a few milliseconds may not pose electromagnetic field transients of greater danger to human beings. This is because the severity level of touch or step potential depends on voltage gradient magnitude, distance and time of exposure.

5. Conclusion

The paper has shown that sag has a direct bearing on overhead line external insulation. The position of largest sag has the largest electromagnetic fields on the ground. This can be a common source of electrical accidents. The absolute values of these fields decrease in amplitude as one move away from the line going in the lateral direction or from mid span section towards the tower on either side. All the essential angles for visualizing electromagnetic wave propagation in the overhead line transmission corridor have been clearly shown.

References

[1] K Rajagopala, K Panduranga Vittal, Hemsingh Lunavath. Computation of Electric Field and Thermal Properties of a 3-Phase Cable. *TELKOMNIKA*. 2012; 10(2): 265-274.
[2] Huang Wang-jun. Modeling and Simulation Research on Lighting Overvoltage of 500 kV Hydroelectric Station. *TELKOMNIKA*. 2012; 10(4): 619-624.
[3] Adel Z, El Dein. *Mitigation of Magnetic Field under Egyptian 500 kV Overhead Transmission Line*. 7th International Multi-Conference on Systems, Signals, and Devices. 2010.
[4] Daochun Huang, Jiangjun Ruan. *Discussion on Electromagnetic Environment of 1000 kV AC Overhead Transmission Lines in China*. The 8th International Power Engineering Conference. IPEC. 2007.
[5] NMK Abdel-Gawad. An Investigation into Field Management under Power Transmission Lines using Delta Configurations. *The Open Environmental Engineering Journal*. 2009; 2.
[6] OBC Miguel, CA Melo Luiz Fonseca, E Fontans, SR Naidu. Electric and Magnetic Fields of Compact Transmission Lines. *IEEE Transactions on Power Delivery*. 1999; 14(1): 200-204.
[7] CJ Durkin, RP Fogarty, TM Halleran, DA Mark, A Mukhopadhyay. Five Years of Magnetic Field Management. *IEEE Transactions on Power Delivery.* 1995; 10(1): 219-228.
[8] Yuan Shangzun, Li Pengfei, Nie Ling. *Study on electromagnetic radiation of ultra-high voltage power transmission line*. International Conference on Computer Science and Information Technology. 2008.
[9] J Bradburg, GF Kuska, DJ Tarr, *Sag and Tension Calculations for Mountainous Terrain*. IEEE Proceedings. 1982; 129(5): 213-220.
[10] Shelley L Chen, WZ Black, Michael L. Fancher. High-Temperature Sag Model for Overhead Conductors. *IEEE Transactions on Power Delivery.* 2003; 18(1): 183-188.
[11] Rakosh Das Begamudre. *Extra High Voltage AC Transmission Engineering*. 3rd edition. New Delhi: New Age International ltd. 2006:1-405.
[12] RE James, Q Su. Co*ndition Assessment of High Voltage Insulation in Power System Equipment*. 1st edition. London:The Institution of Engineering and Technology. 2008; 1-239.